Hindawi Publishing Corporation
Journal of Biomedicine and Biotechnology
Volume 2009, Article ID 201075, 7 pages
doi:10.1155/2009/201075

Research Article

Engineering and Directed Evolution of a Ca^{2+} Binding Site A-Deficient AprE Mutant Reveal an Essential Contribution of the Loop Leu_{75}–Leu_{82} to Enzyme Activity

Eliel R. Romero-García,[1] Alfredo Téllez-Valencia,[2] María F. Trujillo,[1] José G. Sampedro,[2] Hugo Nájera,[3] Arturo Rojo-Domínguez,[3] Jesús García-Soto,[1] and Mario Pedraza-Reyes[1]

[1] *Departamento de Biología, Universidad de Guanajuato, Colonia Noria Alta S/N, Guanajuato, 36050 Guanajuato, Mexico*
[2] *Centro de Investigación en Alimentos y Nutrición, Facultad de Medicina, Universidad Juárez del Estado de Durango, Avenida Universidad y Anitúa S/N, 34000 Durango, Mexico*
[3] *Departamento de Ciencias Naturales, Universidad Autónoma Metropolitana Unidad Cuajimalpa, Pedro Antonio de los Santos 84, San Miguel Chapultepec 11850, Mexico*

Correspondence should be addressed to Mario Pedraza-Reyes, pedrama@quijote.ugto.mx

Received 12 February 2009; Revised 17 May 2009; Accepted 15 June 2009

Recommended by George Makhatadze

An *aprE* mutant from *B. subtilis* 168 lacking the connecting loop Leu_{75}–Leu_{82} which is predicted to encode a Ca^{2+} binding site was constructed. Expression of the mutant gene (*aprEΔLeu*$_{75}$–*Leu*$_{82}$) produced *B. subtilis* colonies lacking protease activity. Intrinsic fluorescence analysis revealed spectral differences between wild-type AprE and AprEΔL_{75}–L_{82}. An AprEΔL_{75}–L_{82} variant with reestablished enzyme activity was selected by directed evolution. The novel mutations Thr_{66}Met/Gly_{102}Asp located in positions which are predicted to be important for catalytic activity were identified in this variant. Although these mutations restored hydrolysis, they had no effect with respect to thermal inactivation of AprEΔL_{75}–L_{82} T_{66}M G_{102}D. These results support the proposal that in addition to function as a calcium binding site, the loop that connects β-sheet e3 with α-helix c plays a structural role on enzyme activity of AprE from *B. subtilis* 168.

1. Introduction

Currently, there is a high level of commercial interest for subtilisins that work under extreme biochemical conditions [1, 2]. Therefore, understanding the structure and function of subtilisins is fundamental to employing rational and directed evolution strategies in order to enhance activity and/or change substrate specificity for these proteins [3, 4]. However, there are structural motifs in subtilisin E (AprE) which have proven to affect enzyme activity and still remain uncharacterized. For instance, crystallographic analysis revealed that residues Leu_{75}, Asn_{77}, Ile_{79}, and Val_{81} located in the connecting loop Leu_{75}–Leu_{82} together with Gln_2 and Asp_{41} form a calcium binding site (CBS) in subtilisin BPN' [5]. Furthermore, it is known that residues Gly_{83}-Ser_{85}, conserved among several members of the subtilisin family [6], form a stretch bend which lies at the C-terminal edge of the loop connecting β-sheet e3 to α-helix c. These residues are located 1.5 nm away from and on the opposite side of the catalytic residues Asp_{32}, His_{64}, and Ser_{221} [7]. Despite their far location from the catalytic residues, mutations in this region induce changes on both substrate specificity and enzyme activity of subtilisins. For instance, a single Ser_{85}Ala mutation increased twice the *kcat* of *B. subtilis* 168 AprE [6], and a Val_{84}Ile mutation not only increased the *Km* of subtilisin BPN' but also adapted the enzyme to work at a lower than normal temperature [7].

Members of the subtilisin family usually possess two calcium binding sites (CBSs), named CBSA and CBSB [8]. Each CBS displays different affinity for the calcium ion [8]. In this report, evidence is presented supporting the idea that in addition to the role as a calcium binding site, the

loop connecting β-sheet e3 with α-helix c (residues Leu_{75}–Leu_{82}) also plays an important role in the enzyme activity of subtilisin E from *B. subtilis* 168.

2. Materials and Methods

2.1. Bacterial Strains, Plasmids, and Growth Conditions. Bacterial strains used in this work are listed in Table 1. The growth medium used routinely was Luria-Bertani (LB) [9]. Preparation of competent *E. coli* and *B. subtilis* cells and their transformations were performed as previously described [10, 11].

2.2. Site-Directed Mutagenesis of AprE. Codons 75 through 82 from wild-type *aprE* [13, 14] were eliminated with the Altered Sites II Site-Directed Mutagenesis System Kit (Promega, Madison, WI) using the oligonucleotide 5′-GCTTGGGCTAACGCC∗AGCGGCAATCGTACC-3 (asterisk denotes the location of the in-frame deletion).

2.3. Random Mutagenesis of AprEΔLeu_{75}–Leu_{82}. Random mutagenesis was carried out as follows. Strain *B. subtilis* PERM570 (Table 1) was grown to an $O.D._{600\,nm}$ of 0.5; the cell culture was supplemented with 2 mM H_2O_2 and incubated for 48 hours at 37°C. Cells were serially diluted, and aliquots of 100 μL were inoculated on LB agar plates supplemented with skimmed milk. The plates were incubated 12 hours at 37°C, and colonies exhibiting caseinolytic activity were selected and transferred to a fresh plate. The plasmids of selected colonies were isolated and used to retransform *B. subtilis* 1A751 and *E. coli* DH5α. The *apr*EΔL_{75}–L_{82} variant generated through this protocol was fully sequenced on both strands.

2.4. Expression and Purification of Wild-Type and AprE Mutants. Wild-type *aprE* and *aprE*ΔL_{75}–L_{82} BamHI/BamHI fragments encoding the preproenzymes were cloned in plasmid pUSH2 [12] to introduce an in-frame six histidine-coding sequence at the 3′ end of both *aprE* sequences. This strategy generated the strains, *E. coli* PERM223 harboring pPERM222 (pUSH2-*aprE*) and *E. coli* PERM494 harboring pPERM494 (pUSH2-*aprE*ΔL_{75}–L_{82}), respectively. Wild-type and AprE variants were expressed and purified from the culture media of *B. subtilis* 1A751 by metal affinity chromatography on a Ni-NTA-agarose column (Quiagen; Valencia, CA) as previously described [6]. Protein concentrations were determined by using the Coomassie (Bradford) Protein Assay Kit (Pierce; Rockford, IL).

2.5. Subtilisin Intrinsic Fluorescence (IF) Assays. Fluorescence spectra data were obtained after equilibration of a mixture containing 4 μM of either wild-type or mutant AprEΔL_{75}–L_{82} in 10 mM Pipes pH 7.5 at 25°C in the presence or absence of 0.5 mM EGTA in a spectrofluorophotometer RF-5301PC (Shimadzu, Japan) equipped with both a thermostated cell and constant stirring. Fluorescence spectra were recorded between 280–450 nm upon exciting the protein at 280 nm.

2.6. Thermal Unfolding Followed by Intrinsic Fluorescence. Subtilisin E samples were placed into a 2 mL quartz cuvette; changes in intrinsic fluorescence were measured at 340 nm using an excitation wavelength of 280 nm (4 nm bandwidth) and emission wavelength from 300 to 400 nm (4 nm bandwidth). Temperature was ramped from 25 to 90°C with a 1°C min^{-1}. Thermal unfolding data were normalized to

$$\alpha = \frac{[y(x) - y(x')]}{[y(x = 298.16) - y(x')]}, \tag{1}$$

where x' is the temperature in Kelvin where the enzyme was completely unfolded. Thermodynamic parameters were calculated by nonlinear least-squares fitting to following scheme.

Two-state model between native (N) and unfolded (U) states $N \rightarrow U$. Data were analyzed using the thermal following equation:

$$F_U = \frac{e^{-(\Delta H_m/RT + \Delta H_m/RT_m)}}{1 + e^{-(\Delta H_m/RT + \Delta H_m/RT_m)}}, \tag{2}$$

where T is temperature in K, T_m is the temperature at midpoint, and ΔH_m is the enthalpy at the T_m, respectively.

2.7. Enzyme Kinetics. The synthetic peptide Succinyl-Ala-Ala-Pro-Phe-*p*-nitroanilide (s-AAPF-*p*-Na, Sigma Chemical Co. St. Louis, MO) was used as substrate; assays were performed in 100 mM Tris-HCl (pH 8.0) and 5 mM $CaCl_2$ at 37°C. The amount of *p*-nitroanilide released was measured by recording the absorbance increase at 410 nm. Enzyme activity was expressed as units/mg protein. Velocity data were fitted to the Michaelis-Menten equation by nonlinear regression.

2.8. Thermal Stability of the Enzymes. Purified wild-type or variant AprE enzymes (0.7 mg/mL) were incubated in 100 mM Tris-HCl (pH 8.0) and varying concentrations of both $CaCl_2$ (100 μM–5 mM) and NaCl (0 or 100 mM). The wild-type and variant AprE were either previously treated or not with 100 μM EDTA and then incubated on ice for 15 minutes before testing for thermal stability. The activity remaining after a given time of incubation was determined at 37°C using s-AAPF-*p*Na as the substrate. The temperatures tested for enzyme stability were between 50–65°C.

2.9. Data Analysis. Thermal inactivation kinetics for both WT and AprE variant were studied fitting the inactivation data to (3) by nonlinear regression and using the iterative program Microcal Origin, as described in studies of thermal enzyme inactivation [15]. The equation used was the following:

$$A_R = A_0 e^{-(k \cdot t)}, \tag{3}$$

where A_R represents the (%) of residual activity at a given time (t), A_0 is the initial relative activity, considered as 100%, and k is the rate constant for enzyme inactivation in min^{-1}. Equation (3) describes a one-step process (4) for enzyme inactivation; from the native (N) to the inactive state (I):

$$N \xrightarrow{k} I. \tag{4}$$

Table 1: Bacterial strains used in this study.

Bacterial strain	Genotype and description	Reference or source
Bacillus subtilis		
168	*trp*C2	W. Nicholson
1A751	*egl*SΔ1*02 bgl*T/*bgl*SΔEV *apr*E *npr*E *his*	BGSC*
PERM222	*B. subtilis* 1A751 containing pPERM222 (1.2 kbp PCR fragment containing wild-type *apr*E ORF subcloned in pUSH2	This study
PERM570	*B. subtilis* 1A751 *egl*SΔ1*02 bgl*T/*bgl*SΔEV *apr*E *npr*E *his mut*M:Tet^r, *mut*Y:Sp^r, *sod*A:Cm^r containing pPERM494 (1.2 kbp *Bam*HI fragment from *aprE*ΔL_{75}–L_{82} cloned in PUSH2)	This study
PERM505	*B. subtilis* 1A751 containing pPERM494 (1.2 kbp *Bam*HI fragment from *aprE*ΔL_{75}–L_{82} cloned in PUSH2)	This study
PERM658	*B. subtilis* 1A751 containing pPERM669 (1.2 kbp *Bam*HI fragment from *aprE*ΔL_{75}–L_{82} T_{66}M G_{102}D cloned in PUSH2)	This study
PERM200	*B. subtilis* 1A751 containing pUSH2 (*E. coli-B. subtilis* shuttle vector for C-terminal $His_{(6)}$-tagging Cm^r, Kan^r [12])	This study

* BGSC: *Bacillus* Genetic Stock Center.

3. Results and Discussion

Mutations in the stretch bend Gly_{83}-Ser_{85} lying at the C-terminal edge of the loop connecting the β-sheet e3 with the α-helix c of AprE led to changes on both substrate specificity and enzyme activity of subtilisins [6, 7]. These findings strongly suggest that this region has an important structural role for enzyme activity in AprE. Therefore, this loop was eliminated by site-directed mutagenesis, and the resulting *aprE*ΔL_{75}–L_{82} mutant gene (Figure 1) was expressed in *B. subtilis* 1A751, a strain lacking protease activity as determined on casein plates (Figure 1). In fact, the cell free culture medium of this strain possessed no activity against hide powder azure and only 3% of the activity showed by the strain expressing the wild-type *aprE* gene against azocasein (Results not shown). A version of subtilisin BPN' lacking the CBSA and containing stabilizing mutations has been previously produced [16, 17]. Refolding of this protein was greatly facilitated by the absence of the Ca-loop while retaining high levels of activity [17]. However, as described here in the absence of stabilizing mutations deletion of the CBSA on AprE resulted in a dramatic loss of enzyme activity. Therefore, the loop L_{75}–L_{82} may be important for structural integrity of not only the binding site but also the active site.

Changes in intrinsic fluorescence are excellent for monitoring the polarity of Trp environment and hence are sensitive to protein conformation [18, 19]. Therefore, the emission fluorescence spectra of AprE and AprEΔL_{75}–L_{82} were recorded with excitation at 280 nm. The AprEΔL_{75}–L_{82} spectrum showed an emission maximum of ~358 nm which was red-shifted by 14 nm relative to the peak of the wild-type AprE spectrum (Figure 2(a)). These data suggest that the side chains of the aromatic residues are more exposed to the solvent in AprEΔL_{75}–L_{82}. Moreover, as shown in Figure 2(a), the peak emission intensity of AprEΔL_{75}–L_{82} is ~1.9-fold higher compared to that of wild-type AprE. A comparative amino acid sequence analysis reveals that AprE

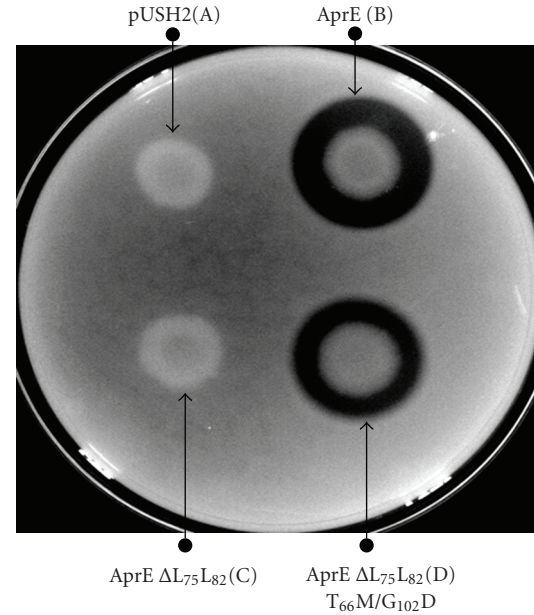

Figure 1: *Extracellular proteolytic activity of strains B. subtilis PERM200 (A), PERM222 (B), PERM505 (C), and PERM658 (D).* 10 μL aliquots were taken from cell cultures (O.D.$_{600\,nm}$ of ~0.5) and deposited on LB agar plates containing 2% (w/v) skimmed milk. The plates were incubated overnight at 37°C to allow the developing of halos of hydrolysis.

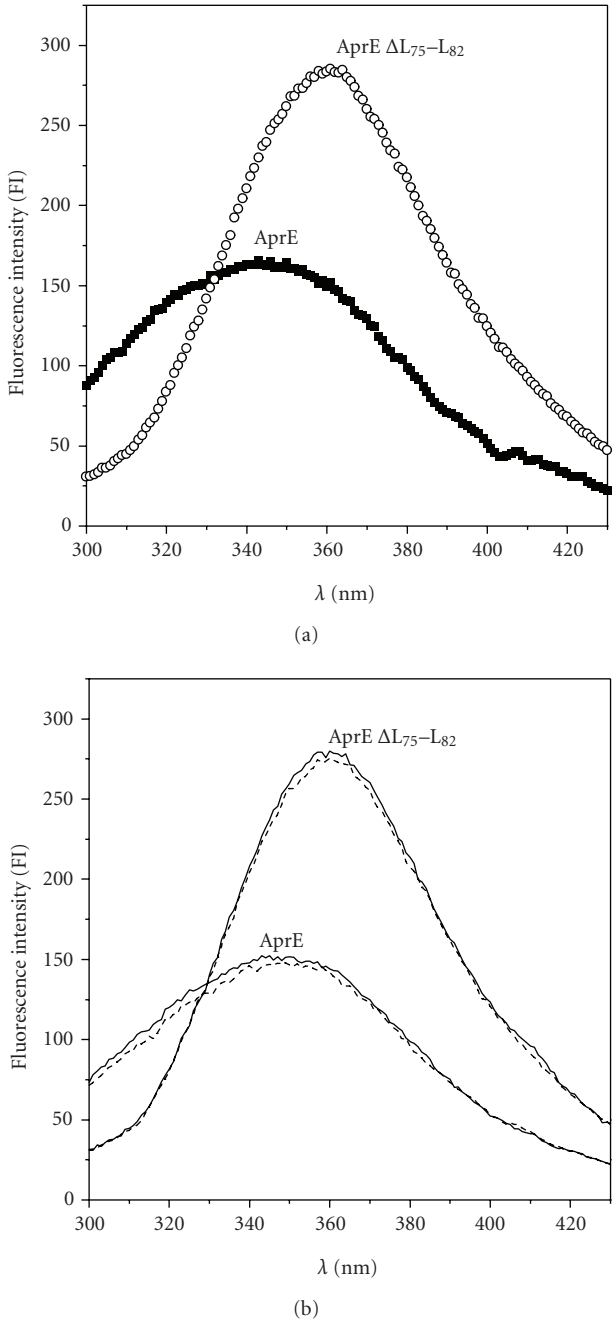

Figure 2: *(a) Emission spectra of wild-type AprE and AprEΔL_{75}–L_{82}.* (Solid squares) wild-type AprE, (Open circles) AprEΔL_{75}–L_{82}. *(b) Emission spectra of wild-type AprE and AprEΔL_{75}–L_{82} in the presence of 0.5 mM EGTA.* (Continuous line) native state; (Dashed line) 0.5 mM EGTA. Assays were performed on 10 mM Pipes, pH 7.5 buffer at room temperature (25°C) using a 1 cm cuvette of 1.5 mL with continuous shaking.

and subtilisin BPN' share 86% similarity; in fact the three tryptophan residues existing in mature subtilisin BPN' (i.e., Trp_{106}, Trp_{113}, and Trp_{241}) are present in equivalent positions in AprE (i.e., Trp residues 105, 112, and 240, resp.) [5, 20, 21]. On the other hand, a previous study suggested that in subtilisin BPN', Trp_{113}, is virtually nonfluorescent; the largely exposed Trp_{241} contributes 20% of the fluorescence, whereas the partially exposed Trp_{106} accounts for the majority of the emission [22]. Therefore, the increased fluorescence intensity observed in AprEΔL_{75}–L_{82} could be attributed to perturbations in the local environment of residues Trp_{105} and/or Trp_{112} which are located near to the deleted loop L_{75}–L_{82}.

As noted above, deletion of the loop 75–82 abolished the calcium binding potential at site A while leaving intact the calcium binding site B. To further investigate this notion, wild-type and mutant AprE proteins were incubated in the presence of 0.5 mM EGTA, a concentration enough to chelate Ca^{2+} only from the CBSB [23]. As shown in Figure 2(b), elimination of Ca^{2+} from CBSB induced in both enzymes a small decrease in their fluorescence intensity with respect to the nontreated native enzymes (Figure 2(b)). These results are in agreement with the presence of an intact CBSB in both the wild-type and the AprEΔL_{75}–L_{82} enzymes.

The structural consequences of loop L_{75}–L_{82} removal from AprE resulted in the lost not only of the CBSA but also of enzyme activity. Therefore, a directed evolution strategy was used to search for amino acid substitutions in the mutant enzyme that could restore enzyme activity. A plasmid containing *aprEΔL_{75}–L_{82}* was expressed in a hypermutagenic strain of *B. subtilis* deficient on the *mutM mutY* and *sodA* genes that also lacked protease activity as described above. After several rounds of mutagenesis for *aprEΔL_{75}–L_{82}*, three colonies exhibiting extracellular protease activity against casein were recovered. The colony with the highest protease activity was selected to further characterize its phenotype; the clone was called *aprEΔL_{75}–L_{82}* Var1. Interestingly, the cell free culture medium of this strain recovered 27% and 65% of the activity exhibited by the strain expressing the wild-type *aprE* gene against hide powder azure and azocasein, respectively (Results not shown).

Analysis of the nucleotide sequence of *aprEΔL_{75}–L_{82}* Var1 revealed the existence of two nonsense mutations that resulted in amino acid substitutions, Thr_{66}Met and Gly_{102}Asp. The mutant gene named *aprEΔL_{75}–$L_{82}T_{66}MG_{102}D$* was cloned in pUSH2, and the resulting construction was expressed in the protease deficient strain *B. subtilis* IA751 (Figure 1). Calculation of kinetic constants *kcat* and *Km* from initial rate measurements of hydrolysis of s-AAPF-*p*Na revealed that the relative catalytic efficiency of AprEΔL_{75}–L_{82}-T_{66}M G_{102}D was of around 7.4% as compared with the wild-type AprE enzyme (Table 2).

In order to understand the effect of these mutations in the structure of the AprEΔL_{75}–L_{82} T_{66}M G_{102}D enzyme, the medium temperature of denaturation (T_m) was calculated for the three enzymes. Results showed that the T_m value of AprEΔL_{75}–L_{82} was around four degrees higher than that of the wild-type protein (Figure 3), indicative of a more stable enzyme. Interestingly, the T_m value of the AprEΔL_{75}–L_{82} T_{66}M G_{102}D mutant was between the T_m values of the AprEΔL_{75}–L_{82} and wild-type enzymes (Figure 3). These results suggest that the stabilities of the two variants are essentially the same.

The CBSA absence and compensatory mutations on the activity of AprEΔL_{75}–L_{82} T_{66}M G_{102}D were determined.

Table 2: Kinetic parameters of AprE and AprEΔL_{75}–L_{82} T_{66}MG_{102}D during hydrolysis of s-AAPF-*p*Na. Reactions were carried out in 100 mM Tris-HCl, pH 8.0, 5 mM $CaCl_2$, at 37°C, using as substrate s-AAPF-*p*Na. Values are triplicate determinations in two separate experiments ± SD.

Enzyme	*Kcat* (s^{-1})	*Km* (mM)	*kcat/Km* (s^{-1} mM^{-1})	% of relative activity
WT AprE	21.8 ± 1.4	1.7 ± 0.2	12.9 ± 0.7	100
AprEΔL_{75}–L_{82} T_{66}M G_{102}D	2.6 ± 0.4	2.7 ± 0.3	0.96 ± 0.6	7.4

Table 3: Thermal inactivation parameters (k_i and $t_{1/2}^*$) of wild-type AprE and AprE**Δ**L_{75}–L_{82} T_{66}M G_{102}D (Var1).

Assay condition	WT k_i (10^{-4} min^{-1})	WT $t_{1/2}$ (min)	Var1 k_i (10^{-4} min^{-1})	Var1 $t_{1/2}$ (min)
5 mM Ca^{2+}, 50°C	8 ± 2	856	51 ± 4	135
0.1 mM Ca^{2+}, 100 mM NaCl, 50°C	130 ± 16	52	2220 ± 141	3.1
0.1 mM EDTA, 100 mM NaCl, 50°C	2700 ± 170	2.6	3255 ± 32	2.1
5 mM Ca^{2+}, 65°C	490 ± 100	14	4550 ± 9	1.5

* $t_{1/2}$ were obtained considering an A_R = 50% and using (3) (Materials and Methods). Enzymes were dissolved in 100 mM Tris-HCl, pH 8.0. Values are triplicate determinations in two separate experiments ± SD.

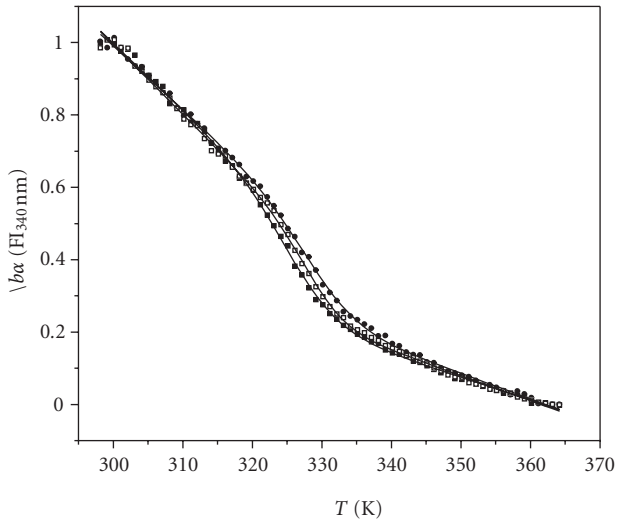

Figure 3: *Thermal unfolding of subtilisin E.* Fluorescence intensity unfolding data for wild-type AprE(■), AprEΔL_{75}–L_{82}(•), and AprEΔL_{75}–L_{82}-T_{66}M G_{102}D (□). The data were obtained with a heating rate of 1 K min^{-1}. Solid lines represent the best fit of unfolding data with ΔHm = 233.3±18.2 kJ mol^{-1} and T_m = 326.9± 0.4 K, ΔHm = 237.3 ± 21.1 kJ mol^{-1} and T_m = 329.8 ± 0.5 K, and ΔHm = 304.5 ± 29.2 kJ mol^{-1} and T_m = 329.3 ± 0.4, respectively.

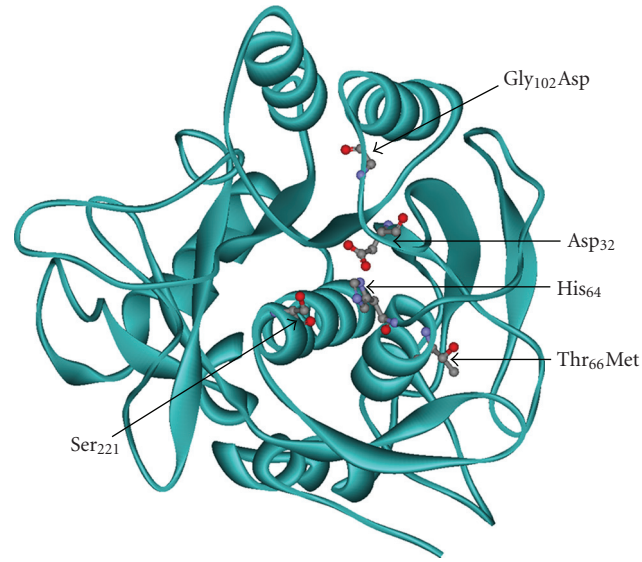

Figure 4: Ribbon diagram of the crystal structure of native subtilisin BPN (from coordinates obtained from [21]), drawn using the program Discovery Studio (http://www.accelerys.com/). Relative locations of the catalytic residues and mutations are indicated.

To this end, AprE and AprEΔL_{75}–L_{82} T_{66}M G_{102}D were incubated with 0.1 mM Ca^{2+} and 100 mM Na^+, respectively. Under these incubation conditions, binding sites A and B of subtilisin BPN' were saturated 95% with Ca^{2+} and Na^+, respectively [24]. The kinetic parameters for thermal inactivation were calculated using (3) to better correlate the effect of amino acid residues substitutions ($Thre_{66}$Met and Gly_{102}Asp) on the calcium dependent stability of AprEΔL_{75}–L_{82}. Table 3 shows that at 50°C and Ca^{2+} saturation, the wild-type AprE enzyme had a $t_{1/2}$ (half life) of 856 minutes. This value is six times higher than that of the AprEΔL_{75}–L_{82} T_{66}M G_{102}D mutant. At 65°C and Ca^{2+} saturation the half life of AprE was 9 times higher than that of AprEΔL_{75}–L_{82} T_{66}M G_{102}D (Table 3). On the other hand, in the presence of 0.1 mM Ca^{2+}, the $t_{1/2}$ for the wild-type enzyme was around 17 times higher than that of the mutant enzyme. However, in the presence of 0.1 mM EDTA, that is, in the absence of calcium, both enzymes showed a similar inactivation rate (Table 3). Therefore amino acid residues substitutions ($Thre_{66}$Met and Gly_{102}Asp) led to recover of enzyme activity but had no effect with respect to thermal inactivation of AprEΔL_{75}–L_{82}.

The three-dimensional structure of AprE has not been determined but it has been reported for subtilisin BPN' [21]. In fact, as noted above both proteins share 86% identity; therefore their three-dimensional structures are likely to be similar. Thus, the structural analysis using subtilisin BPN' as a model [21] revealed that the mutation Thr_{66}Met was found to be in close contact with the active site of the enzyme, in particular interacting with His_{64} which acts as a general-base catalyst to activate the γ-OH group of the nucleophile Ser_{221}. On the other hand, the mutation Gly_{102}Asp was found to occur in the substrate binding subsite S_4 of AprE (Figure 4).

The bulky and nonpolar functional side group of Met suggests that the microenvironment in the active site of the AprEΔL_{75}–L_{82} mutant was disturbed as a consequence of a polarity change. This alteration may impair the nonpolar residues present in the substrate s-AAPF-*p*Na (i.e., Phe) that enter in contact with the catalytic residues. Thus, substitution of Thr_{66}Met possibly had a positive effect in reestablishing the core environment (polarity) in the active site of AprEΔL_{75}–L_{82}. Mutations directed to this region might be useful in identifying amino acid substitutions that reestablish the full activity to AprEΔL_{75}–L_{82}. On the other hand, it has been reported that substitutions of the residues Gly_{102}Phe and Ser_{128}Phe in savinase, a subtilisin ortholog, blocked the entrance of aromatic residues into the active site pocket, eliminating thus the preference for these residues [25]. Therefore, the introduction of a polar and bulky residue like Asp in position 102 of AprEΔL_{75}–L_{82} may anticipate an important structural change in the affinity for the substrate.

Overall, the results of the structural and biochemical analysis of the wild-type, AprEΔL_{75}–L_{82} and AprEΔL_{75}–L_{82} T_{66}M G_{102}D proteins, strongly suggest that the local perturbation induced by deletion of the loop L_{75}–L_{82} were partially compensated by the substitutions T_{66}M G_{102}D which are located in close vicinity with the catalytic triad of AprE. Therefore, the results described in this work strongly support the idea that in addition to function as a Ca^{2+} binding domain, the loopL_{75}–L_{82} has an important structural role in the enzyme activity of AprE.

Acknowledgments

This work was supported by Grants 43644 and 84482 from the Consejo Nacional de Ciencia y Tecnología (CONACYT) of México to Mario Pedraza-Reyes. Eliel R. Romero-García and María F. Trujillo were supported by fellowships from CONACYT. We wish to thank Ronald E. Yasbin for critical review of this manuscript and to Sivia J. Mellado for excellent technical assistance.

References

[1] Y. Yang, L. Jiang, L. Zhu, Y. Wu, and S. Yang, "Thermal stable and oxidation-resistant variant of subtilisin E," *Journal of Biotechnology*, vol. 81, no. 2-3, pp. 113–118, 2000.

[2] H. Zhao and F. H. Arnold, "Directed evolution converts subtilisin E into a functional equivalent of thermitase," *Protein Engineering*, vol. 12, no. 1, pp. 47–53, 1999.

[3] P. N. Bryan, "Protein engineering of subtilisin," *Biochimica et Biophysica Acta*, vol. 1543, no. 2, pp. 203–222, 2000.

[4] S. L. Strausberg, P. A. Alexander, D. T. Gallagher, G. L. Gilliland, B. L. Barnett, and P. N. Bryan, "Directed evolution of a subtilisin with calcium-independent stability," *Biotechnology*, vol. 13, no. 7, pp. 669–673, 1995.

[5] S. C. Jain, U. Shinde, Y. Li, M. Inouye, and H. M. Berman, "The crystal structure of an autoprocessed Ser221Cys-subtilisin E-propeptide complex at 2.0 A resolution," *Journal of Molecular Biology*, vol. 284, no. 1, pp. 137–144, 1998.

[6] E. R. Romero-Garcia, J. A. Esquivel-Naranjo, N. Ramirez-Ramirez, J. Garcia-Soto, and M. Pedraza-Reyes, "A single Ser_{85}Ala mutation enhances the catalytic efficiency of subtilisin E from *Bacillus subtilis* 168," *Biotechnology*, vol. 3, pp. 49–55, 2004.

[7] H. Kano, S. Taguchi, and H. Momose, "Cold adaptation of a mesophilic serine protease, subtilisin, by in vitro random mutagenesis," *Applied Microbiology and Biotechnology*, vol. 47, no. 1, pp. 46–51, 1997.

[8] P. A. Alexander, B. Ruan, and P. N. Bryan, "Cation-dependent stability of subtilisin," *Biochemistry*, vol. 40, no. 35, pp. 10634–10639, 2001.

[9] J. H. Miller, *Experiments in Molecular Genetics*, Cold Spring Harbor Laboratory Press, Cold Spring Harbor, NY, USA, 1972.

[10] R. J. Boylan, N. H. Mendelson, D. Brooks, and F. E. Young, "Regulation of the bacterial cell wall: analysis of a mutant of *Bacillus subtilis* defective in biosynthesis of teichoic acid," *Journal of Bacteriology*, vol. 110, no. 1, pp. 281–290, 1972.

[11] J. Sambrook, E. F. Fritsch, and T. Maniatis, *Molecular Cloning: A Laboratory Manual*, Cold Spring Harbor Laboratory Press, Cold Spring Harbor, NY, USA, 2nd edition, 1989.

[12] U. Schön and W. Schumann, "Construction of His_6-tagging vectors allowing single-step purification of GroES and other polypeptides produced in *Bacillus subtilis*," *Gene*, vol. 147, no. 1, pp. 91–94, 1994.

[13] F. Kunst, N. Ogasawara, I. Moszer, et al., "The complete genome sequence of the gram-positive bacterium *Bacillus subtilis*," *Nature*, vol. 390, no. 6657, pp. 249–256, 1997.

[14] M. L. Stahl and E. Ferrari, "Replacement of the *Bacillus subtilis* subtilisin structural gene with an in vitro-derived deletion mutation," *Journal of Bacteriology*, vol. 158, no. 2, pp. 411–418, 1984.

[15] J. G. Sampedro, P. Cortes, R. A. Muñoz-Clares, A. Fernández, and S. Uribe, "Thermal inactivation of the plasma membrane H+-ATPase from *Kluyveromyces lactis*. Protection by trehalose," *Biochimica et Biophysica Acta*, vol. 1544, no. 1-2, pp. 64–73, 2001.

[16] T. Gallagher, P. Bryan, and G. L. Gilliland, "Calcium-independent subtilisin by design," *Proteins*, vol. 16, no. 2, pp. 205–213, 1993.

[17] O. Almog, T. Gallagher, M. Tordova, J. Hoskins, P. Bryan, and G. L. Gilliland, "Crystal structure of calcium-independent subtilisin BPN' with restored thermal stability folded without the prodomain," *Proteins*, vol. 31, no. 1, pp. 21–32, 1998.

[18] J. R. Lacowicz, "Fluorophores," in *Principles of Fluorescence Spectroscopy*, J. R. Lacowicz, Ed., pp. 63–93, Kluwer Academic/Plenum Publishers, New York, NY, USA, 1999.

[19] G. S. Lakshmikanth and G. Krishnamoorthy, "Solvent-exposed trytophans probe the dynamics at protein surfaces," *Biophysical Journal*, vol. 77, no. 2, pp. 1100–1106, 1999.

[20] F. S. Markland Jr. and E. L. Smith, "Subtilisins: Primary Structure, Chemical and Physical Properties," in *The Enzymes*, P. D. Boyer, Ed., pp. 561–608, Academic Press, New York, NY, USA, 1971.

[21] T. Gallagher, J. Oliver, R. Bott, C. Betzel, and G. L. Gilliland, "Subtilisin BPN' at 1.6 A resolution: analysis for discrete disorder and comparison of crystal forms," *Acta Crystallographica Section D*, vol. 52, no. 6, pp. 1125–1135, 1996.

[22] M. Shopova and N. Genov, "Protonated form of histidine 238 quenches the fluorescence of tryptophan 241 in subtilisin Novo," *International Journal of Peptide and Protein Research*, vol. 21, no. 5, pp. 475–478, 1983.

[23] R. D. Kidd, H. P. Yennawar, P. Sears, C.-H. Wong, and G. K. Farber, "A weak calcium binding site in subtilisin BPN' has a dramatic effect on protein stability," *Journal of the American Chemical Society*, vol. 118, no. 7, pp. 1645–1650, 1996.

[24] P. A. Alexander, B. Ruan, S. L. Strausberg, and P. N. Bryan, "Stabilizing mutations and calcium-dependent stability of subtilisin," *Biochemistry*, vol. 40, no. 35, pp. 10640–10644, 2001.

[25] L. M. Bech, S. B. Sørensen, and K. Breddam, "Significance of hydrophobic S4-P4 interactions in subtilisin 309 from *Bacillus lentus*," *Biochemistry*, vol. 32, no. 11, pp. 2845–2852, 1993.